XXX manuscript No.
(will be inserted by the editor)

M. I. Dolz[1] · **P. Pedrazzini**[2] · **H. Pastoriza**[2] ·
M. Konczykowski[3] · **Y. Fasano**[2]

Effect of quenched disorder in the entropy-jump at the first-order vortex phase transition of $Bi_2Sr_2CaCu_2O_{8+\delta}$

May 4, 2015

Abstract We study the effect of quenched disorder in the thermodynamic magnitudes entailed in the first-order vortex phase transition of the extremely layered $Bi_2Sr_2CaCu_2O_{8+\delta}$ compound. We track the temperature-evolution of the enthalpy and the entropy-jump at the vortex solidification transition by means of AC local magnetic measurements. Quenched disorder is introduced to the pristine samples by means of heavy-ion irradiation with Pb and Xe producing a random columnar-track pins distribution with different densities (matching field B_Φ). In contrast with previous magneto-optical reports, we find that the first-order phase transition persists for samples with B_Φ up to 100 Gauss. For very low densities of quenched disorder (pristine samples), the evolution of the thermodynamic properties can be satisfactorily explained considering a negligible effect of pinning and only electromagnetic coupling between pancake vortices lying in adjacent CuO planes. This description is not satisfactory on increasing magnitude of quenched disorder.

1 Introduction

The vortex solidification or first-order phase transition (FOT) [1,2] dominates the magnetic phase diagram of pristine samples of anisotropic high-temperature superconductors. The location of the FOT line and the temperature-evolution of the thermodynamic magnitudes at the transition are given by the balance between thermal, vortex-quenched disorder and inter-vortex interaction energies. All these terms are strongly dependent on the anisotropy parameter of the material that determines the degree of layerness of vortex matter. In the case of the extremely-anisotropic $Bi_2Sr_2CaCu_2O_8$ compound, when applying a field along the c-axis individual vortices are composed of a stack of pancake vortices lying in CuO planes.

1: Departamento de Física, Universidad Nacional de San Luis, CONICET, Argentina
2: Low Temperature Division, Centro Atómico Bariloche, CNEA, Argentina
3: Laboratoire des Solides Irradiés, Ecole Polytechnique, Palaiseau, France
Corresponding author: E-mail: mdolz@unsl.edu.ar

Within one vortex line, pancake vortices couple between layers due to electromagnetic and Josephson interactions[3]. For temperatures $T < T_{FOT}$ the stable phase in this compound is a vortex solid with quasi long-range transversal positional order[4,5] and long-range coupling between the pancake vortices concatenating a flux quantum. At the transition temperature T_{FOT}, a decoupling process of pancake vortices from adjacent layers takes place within the same stack[6]. There is still some controversy as to whether the high-temperature phase is a liquid[7] or a decoupled gas[8] of pancake vortices with reduced shear viscosity[9].

Nevertheless, the FOT is a single-vortex transition in which the relative importance of the two types of interactions between pancake vortices determine the location of the T_{FOT} line[3]. Previous works on pristine samples found a sudden decrease of enthalpy and a divergence of the entropy for $T_{FOT} \sim T_c$ by applying DC and AC magnetometry[2,10]. These results were theoretically interpreted as due to the Josephson interlaying coupling playing a determinant role when the temperature of the transition approaches T_c[11]. This theoretical study does not take into account the effect of the vortex-quenched disorder interaction (pinning) that plays a relevant role in most cases.

Indeed, the magnitude of quenched disorder is a control parameter that significantly affects the location of the FOT line. A largely used method to introduce disorder with different magnitude is the irradiation of samples with heavy ions resulting in the creation of columnar tracks or defects (CD)[12]. This method generates a random distribution of strong pinning centers with a density that can be adjusted by the irradiation dose. The density of CDs is normally expressed in units of matching fields, $B_\Phi = \Phi_0/a_{CD}^2$, with a_{CD} the average spacing between tracks. Heavy-ion-irradiated $Bi_2Sr_2CaCu_2O_8$ samples with a low density of CDs present a solid vortex phase that spans a larger temperature-region on increasing the magnitude of quenched disorder[13,14]. Previous magneto-optical measurements indicate the transition to the high-temperature phase is no longer of first-order for matching fields of roughly 100 Gauss[13,14]. In the latter case, a continuous change in the sample local induction is observed on crossing the vortex solidification line, in contrast to the sudden jump in B detected for pristine samples.

In this work we study the main thermodynamic magnitudes entailed in the vortex solidification transition of $Bi_2Sr_2CaCu_2O_8$ by means of local AC magnetometry. We investigate the nature of the transition on increasing the density of quenched disorder in one order of magnitude, $B_\Phi = 10$ and 100 Gauss for samples irradiated with Xe and Pb ions. We focus on the effect of the magnitude of disorder (directly proportional to the density of CDs) on the entropy-jump, ΔS, and on the enthalpy of the transition, proportional to ΔB.

2 Experimental

The nearly optimally-doped $Bi_2Sr_2CaCu_2O_8$ single-crystals used in this work were grown by means of the traveling-solvent floating zone technique as discused in Ref. [15]. The samples were irradiated with Pb and Xe heavy-ions at Ganil, France. In this study we measure a pristine sample, a Xe-irradiated sample with $B_\Phi = 10$ Gauss, and a Pb-irradiated sample with $B_\Phi = 100$ Gauss. The samples were mounted onto 2D-electron-gas Hall-sensor arrays photolithographically fabricated from GaAs/AlGaAs heterostructures. Each sensor has an active area of

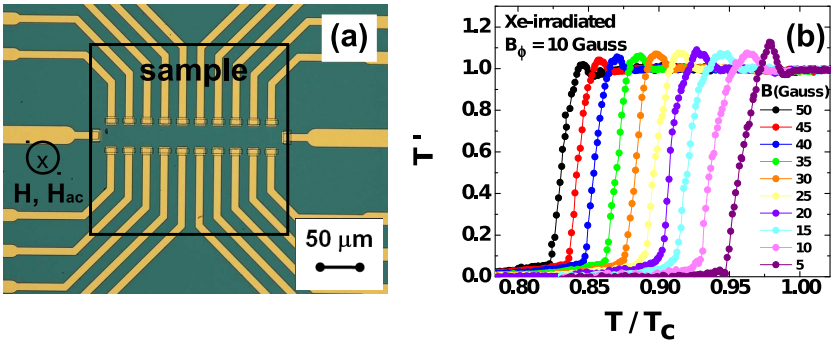

Fig. 1 (a) Schematics of the experimental configuration: picture of one of the 11-probe Hall arrays used for the AC magnetometry measurements with a in-scale representation of the sample size and location. The direction of the DC and AC fields with respect to the sample and Hall probe are indicated. (b) Temperature-evolution of the transmittivity for different applied fields in the case of the Xe-irradiated $Bi_2Sr_2CaCu_2O_8$ sample. The AC ripple field used for this measurements had a magnitude of 2 Gauss and a frequency of 7 Hz. (color figure online).

$6 \times 6\,\mu\mathrm{m}^2$ and samples have typical areas of $200 \times 200\,\mu\mathrm{m}^2$ and thickness of 30-50 μm. DC and AC-ripple magnetic fields, H and H_{ac}, are applied parallel to the c-axis of the samples, namely perpendicular to the Hall probe surface. The AC ripple fields have magnitudes of 1-2 Gauss and frequencies up to 15 Hz. For all studied samples the response of the vortex system to this AC excitation is within the linear Campbell regime. A schematic representation of the measurement configuration for one of the probes used is shown in Fig. 1 (a).

The local magnetic response was characterized by measuring the first harmonic of the AC induction by means of a digital-signal-processing lock-in technique[16]. We obtained the transmittivity by normalizing the in-phase component of the first harmonic signal as $T' = [B'(T) - B'(T \ll T_{\mathrm{c}})]/[B'(T > T_{\mathrm{c}}) - B'(T \ll T_{\mathrm{c}})]$[17]. This magnitude is extremely sensitive to discontinuities in the local induction associated to first-order magnetic transitions. In order to track the $H - T$ location of the solidification transition in $Bi_2Sr_2CaCu_2O_8$ vortex matter we measured T' as a function of temperature for various DC applied fields.

3 Results and discussion

Figure 1 (b) shows a set of transmittivity data for the Xe-irradiated sample with $B_\Phi = 10$ Gauss and DC fields ranging from 5 to 50 Gauss. The so-called paramagnetic peak observed in the curves is considered as the fingerprint of the first-order vortex solidification transition since it develops at the same T_{FOT} as the jump in B detected in DC hysteresis loops[10]. In addition, the temperature-location of this paramagnetic peak is frequency-independent. The T_{FOT} temperature, taken at the maximum of the peak, shifts towards lower temperatures on increasing field. The peaks are sharp and have an amplitude that slightly decreases on increasing field. The same field and temperature evolution was observed for pristine as well as the Pb and Xe-irradiated samples.

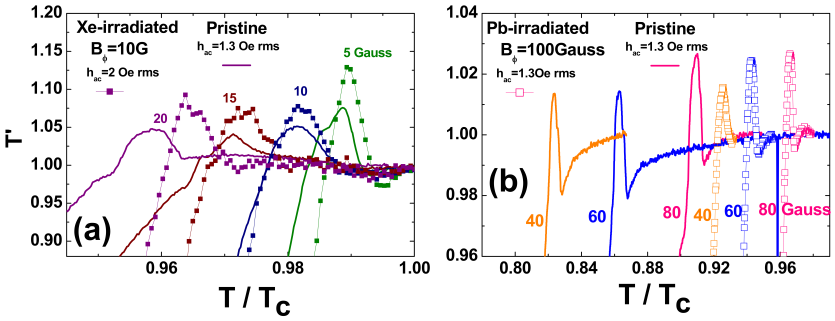

Fig. 2 Temperature-evolution of the transmittivity for low fields for irradiated in comparison to pristine $Bi_2Sr_2CaCu_2O_8$ samples: (a) Xe-irradiated ($B_\Phi = 10$ Gauss) and (b) Pb-irradiated ($B_\Phi = 100$ Gauss) samples. The amplitudes of the AC ripple fields are as indicated and the frequency is of 7 Hz. (color figure online).

Figure 2 (a) shows, in accordance with the literature, that introducing a small amount of quenched disorder by means of heavy-ion irradiation spans the solid vortex phase in a larger temperature region. This is observed in the T' measurements showing a shifting of the paramagnetic peak towards higher T/T_c in the case of Xe-irradiated $B_\Phi = 10$ Gauss with respect to pristine samples. Figure 2 (b) shows one of the main results of this work: The FOT persists for a larger amount of quenched disorder corresponding to $B_\Phi = 100$ Gauss, in contrast to magneto-optical results [13,14]. The paramagnetic peaks in the Pb-irradiated $B_\Phi = 100$ sample are detected up to more than 100 Gauss and shift towards higher T/T_c in comparison to the pristine sample for a fixed applied field. For instance, in this sample, the solid vortex phase spans a T/T_c region 20% larger than for the pristine sample at 100 Gauss (see insert to Fig. 3 (b)). The discrepancy between our data and previous one has its origin in the local induction resolution in both experiments, being not better than 1 Gauss for magneto-optics data and of the order of 5 mGauss in our AC magnetometry measurements.

The jump in B entailed in the FOT can be obtained from AC measurements taking into account that for $T \gtrsim T_{\rm FOT}$ the transmittivity $T' \sim B'/H_{\rm ac}$. Following thermodynamic considerations as in Ref. [10], and considering that the magnitude of $H_{\rm ac}$ is small, the transmittivity can be approximated by $T'(T_{\rm FOT}) = 1 + \frac{2\Delta B}{\pi H_{\rm ac}}$. Inverting this equation allows the determination of ΔB as a function of $T_{\rm FOT}/T_c$ as shown in Fig. 3 (a). It is important to point out that the value of ΔB obtained in this way is equal to the obtained in DC magnetization loops [10,16]. In the case of the pristine and $B_\Phi = 10$ Gauss samples ΔB increases roughly linearly up to $T_{FOT} \sim T_c$ within the error bars. For the $B_\Phi = 100$ Gauss sample the data do not follow this linear evolution, particularly at low temperatures. A theoretical work [11] predicted a linear evolution of ΔB by considering that the inter-layer coupling is only dominated by electromagnetic interactions between pancake vortices undergoing large thermal fluctuations in a material with negligible pinning. This work proposed that

$$\Delta B = \mu' \frac{k_{\rm B} T_{\rm FOT}}{\Phi_0 d},$$

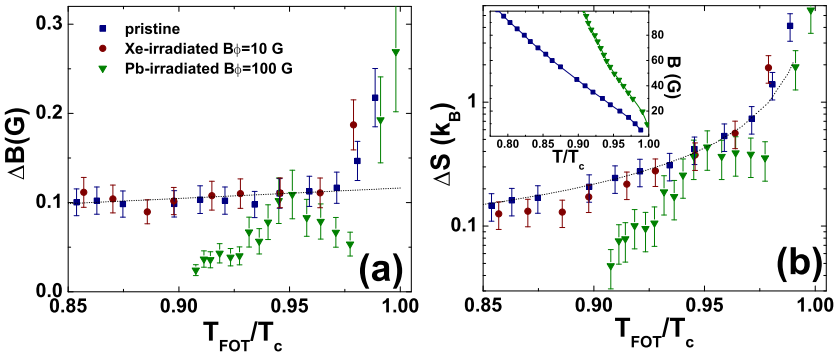

Fig. 3 Reduced-temperature evolution of the (a) enthalpy $\propto \Delta B$ and (b) entropy ΔS at the first-order vortex solidification transition for pristine as well as Xe and Pb-irradiated samples. The full lines are fits to the data with a theoretical model that only takes into account electromagnetic coupling between pancake vortices at the transition (see text). Insert: vortex phase diagram of the samples. (color figure online).

where $k_{\rm B}$ is the Boltzmann constant, Φ_0 the flux quantum, $d \approx 15\AA$ the distance between CuO planes and μ' a numerical constant. The results in the pristine and $B_\Phi = 10$ Gauss samples are reasonably well fitted with this functionality, in contrast to the case of the $B_\Phi = 100$ Gauss sample.

A non-linear evolution of ΔB was previously reported for a pristine $Bi_2Sr_2CaCu_2O_8$ sample in Ref. [2], with this magnitude decreasing to a quarter of its low-temperature value for $T_{\rm FOT}/T_{\rm c} \geq 0.93$. The mentioned theoretical work interpreted this as an indication that electromagnetic interactions alone cannot account for the location of the FOT line close to $T_{\rm c}$ and therefore suggested a crossover to a Josephson-coupling regime [11]. Our ΔB data depart from the linear behavior at low temperatures when the magnitude of quenched disorder is increased. Since the theoretical proposal does not take into account the effect of pinning, our results in pristine and irradiated samples challenge the existence of such a crossover.

The entropy-jump at $T_{\rm FOT}$ obtained from the Clausius-Clapeyron relation is

$$\Delta S = -\frac{\phi_0 d}{4\pi}\frac{\Delta B}{B_{\rm FOT}}\frac{dH_{\rm FOT}}{dT}.$$

Figure 3 (b) shows that the ΔS entailed in the vortex solidification FOT diverges for $T \sim T_{\rm c}$ for pristine as well as for irradiated $Bi_2Sr_2CaCu_2O_8$ samples. Applying the same thermodynamic relation to obtain the entropy of the theoretical system that only takes into account electromagnetic coupling holds

$$\Delta S = \frac{\mu}{\pi}\frac{k_{\rm B}}{[1-(T_{\rm FOT}/T_{\rm c})^2]}.$$

The fit of our experimental data with this function is shown with the dotted line of Fig. 3. Note that this function has only one fitting parameter, the multiplicative constant μ. The ΔS values for the pristine sample follow this theoretical functionality but apart from it on increasing the magnitude of quenched disorder. The fact that this departure between the experimental data and the theoretical model

happens at low temperatures is also at odds with ascribing it to a crossover to Josephson-dominated coupling.

4 Conclusions

Our main result of the persistence of the FOT for $B_\Phi = 100$ Gauss calls for a revision of the nature of the vortex solidification transition in the case of extremely-layered superconducting samples with a moderate magnitude of quenched disorder. Our findings do not challenge the accepted picture of a change from first to second-order transition through a critical point for high-fields or alternatively high-magnitude of quenched disorder. However we put in evidence that the fields and B_Φ for which these critical points occur have to be re-examined by means of local magnetic techniques with improved resolution. In addition, the departure of the enthalpy of the transition from a linear behavior in $T_{\rm FOT}/T_{\rm c}$ when increasing the magnitude of quenched disorder suggests that it is not straightforward to ascribe this phenomenology to a crossover between an electromagnetic-to-Josephson coupling of pancake vortices. A theoretical description taking also into account the effect of pinning is therefore required in order to properly describe the evolution of the thermodynamic magnitudes in the first-order vortex solidification transition.

References

1. H. Pastoriza *et al.*, Phys. Rev. Lett. **72**, 2951 (1994).
2. E. Zeldov *et al.*, Nature **375**, 373 (1995).
3. G. Blatter *et al.*, Rev. Mod. Phys. **66**, 1125 (1994)
4. Y. Fasano, J. Herbsommer, and F. de la Cruz, Phys. Stat. Sol. (b) **215**, 563 (1999).
5. Y. Fasano, and M. Menghini, Supercond. Sc. and Tech. **21**, 023001 (2008).
6. S. Colson,*et al.*, Phys. Rev. Lett. **90**, 137002 (2003).
7. D. R. Nelson, Phys. Rev. Lett. **60**, 1973 (1988).
8. L. I. Glazman and A. E. Koshelev, Phys. Rev. B **43**, 2835 (1991).
9. H. Pastoriza and P. H. Kes, Phys. Rev. Lett. **75**, 3525 (1995).
10. N. Morozov, E. Zeldov, D. Majer and M. Konczykowski, Phys. Rev. B **54**, R3784 (1996).
11. M.J.W. Dodgson, V.B Geshkenbein, H. Nordborg, and G. Blatter, Phys. Rev. Lett. **80**, 837 (1998).
12. L. Civale, Supercond. Sci. Technol. **10**, 11 (1997).
13. S. S. Banerjee *et al.*, Phys. Rev. Lett. **90**, 87004 (2003).
14. M. Menghini *et al.*, Phys. Rev. Lett. **90**, 147001 (2003).
15. T. W. Li *et al.* J. Cryst. Growth **135**, 481 (1994).
16. M. I. Dolz, *et al.*, condmat:1405.4221 (2014).
17. J. Gilchrist, and M. Konczykowski, Phys. C **212**, 43 (1993).